Biophysical Chemistry 154 (2011) 73–81

Contents lists available at ScienceDirect

Biophysical Chemistry

journal homepage: http://www.elsevier.com/locate/biophyschem

Effects of oligomeric lysozyme on structural state of model membranes

Galyna Gorbenko *, Valeriya Trusova

Department of Biological and Medical Physics, V.N. Karazin Kharkov National University, 4 Svobody Sq., Kharkov 61077, Ukraine

ARTICLE INFO

Article history:
Received 4 October 2010
Received in revised form 12 January 2011
Accepted 14 January 2011
Available online 3 February 2011

Keywords:
Lysozyme oligomers
Protein–lipid interactions
Fluorescent probes
Membrane hydration
Pyrene excimer formation
Bilayer free volume

ABSTRACT

The ability of oligomeric lysozyme to modify the molecular organization of the model bilayer membranes composed of phosphatidylcholine (PC) and its mixtures with phosphatidylglycerol (PG) or cholesterol (Chol) was assessed using fluorescent probes 6-propionyl-2-dimethylaminonaphthalene (Prodan), 4-dimethylaminochalcone (DMC), pyrene and 1,6-diphenyl-1,3,5-hexatriene (DPH). The observed changes in the fluorescence characteristics of polarity-sensitive probes Prodan and DMC, located in interfacial bilayer region, were interpreted due to the partial dehydration of the glycerol backbone, which was under the influence of aggregated protein. Cholesterol was found to prevent the perturbations of membrane polar part by lysozyme aggregates. Analysis of the pyrene excimerization data revealed an oligomer-induced reduction in bilayer free volume, presumably caused by an increased packing density of hydrocarbon chains. This effect proved to be virtually independent of membrane composition. It was demonstrated that membranotropic activity of oligomeric lysozyme markedly exceeds that of monomeric protein. The biological significance of the results obtained is twofold, implicating the general membrane-mediated mechanisms of oligomer toxicity and specific pathways of lysozyme fibrillogenesis in vivo associated with familial nonneuropathic systemic amyloidosis.

1. Introduction

Over the past decade the process of abnormal protein aggregation into highly ordered beta-sheet fibrillar structures (amyloids) attracts ever growing interest due to its involvement in molecular etiology of a number of the so-called protein misfolding disorders, including neurodegenerative diseases, type II diabetes, rheumatoid arthritis, etc. Although a consensus about a causative link between amyloid formation and disease has long been reached, the specific nature of the toxic species and molecular details of cell damage by pathogenic protein aggregates are still the subject of intense debate [1]. A central role of early oligomeric intermediates, rather than mature fibrils, in impairment of cell structure and function has been recognized [1,2]. A number of hypotheses have been proposed to explain the structural and biochemical bases of amyloid toxicity. According to a 'channel hypothesis,' cytotoxicity originates from the interactions between misfolded protein species and cellular membranes, followed by the formation of non-specific ion channels [3]. Other hypotheses, explaining the impairment of cell function by pre-fibrillar aggregates in terms of modifications of intracellular redox status and free calcium level [4–6] or uptake of lipids into growing fiber [7], also highlight membrane destabilization as an essential determinant of amyloid cytotoxicity. Furthermore, cell membrane has been assumed to provide a template for nucleation of amyloid fibrils [8,9]. In view of the putative crucial role of membranes in triggering amyloid growth and subsequent cell damage, amyloid-related aspects of protein–lipid interactions acquire special importance. One of such aspects concerns the interactions between oligomeric protein species and lipids. This issue has been addressed in a number of recent studies involving a variety of experimental approaches, viz. AFM [10], infrared reflection absorption spectroscopy [11], surface plasmon resonance [12], small angle neutron scattering [13], circular dichroism [14], fluorescence spectroscopy [15], micropipette manipulation [16], conductivity measurements [17], and dye release assay [18]. The main conclusions reached from the studies of model membrane systems and natural membranes can be briefly outlined as follows:

i) Oligomeric species display much higher affinity for lipid bilayers than mature fibrils, as was demonstrated, particularly, for α-synuclein [10,12], N-terminal domain of the hydrogenase maturation factor HypF-N [19,20] and stefin B [21].
ii) Early oligomers are capable of inducing membrane permeabilization via pore-like mechanisms, as was suggested for IAPP, Aβ-peptide, α-synuclein [14], and HypF-N [19].

Abbreviations: PC, 1-palmitoyl −2-oleoyl-*sn*-glycero-3-phosphocholine; PG, 1-palmitoyl-2-oleoyl-*sn*-glycero-3-phospho-*rac*-glycerol; Chol, cholesterol; Prodan, 6-propionyl-2-dimethylaminonaphthalene; DMC, 4-dimethylaminochalcone; ThT, Thioflavin T; DPH, 1,6-diphenyl-1,3,5-hexatriene; DSP-12, 4-p-(dimethylaminostyryl)-1-dodecylpyridinium; bis-ANS, bis[4.4'-(8-anilino-1-naphthalenesulfonate).

* Corresponding author at: 52–52 Tobolskaya Str., Kharkov 61072, Ukraine. Tel.: +38 057 343 82 44.
E-mail address: galyna.p.gorbenko@univer.kharkov.ua (G. Gorbenko).

0301-4622/$ – see front matter © 2011 Elsevier B.V. All rights reserved.
doi:10.1016/j.bpc.2011.01.003

iii) Oligomeric intermediates give rise to disruption of bilayer integrity and membrane thinning, as was shown, for instance, for α-synuclein [18], Aβ-peptide [13] and HypF-N [20].

Despite great advances in the understanding of oligomer–membrane interactions, little is known about the driving forces and molecular-scale details of this process. In the present study we focused our efforts on the characterization of membrane-modifying properties of oligomeric lysozyme, a multifunctional protein with bactericidal, antitumor and immunomodulatory activities, whose amyloidogenesis in vivo is associated with familial nonneuropathic systemic amyloidosis, a disease in which aggregated protein tends to form deposits in liver, kidneys, and spleen [22].

Several lines of evidence indicate that monomeric lysozyme displays pronounced ability to interact with membranes both electrostatically and hydrophobically, producing a reduction in electrostatic surface potential of the lipid bilayer [23], membrane dehydration [24], and increase of lipid packing density [25]. A question arises, how is membrane modification induced by lysozyme oligomers similar or different from that evoked by its monomers? In an attempt to approach this question, we employed a fluorescent probe technique to compare membrane effects of oligomeric and monomeric lysozyme in the liposomal model systems of varying composition. Shedding light on this problem seems to be of importance not only for elucidating the general mechanisms by which toxic oligomeric species exert destabilizing influence on the membrane structure, but also for gaining deeper insights into lysozyme amyloidogenesis per se. To monitor lysozyme-induced changes in physicochemical properties and molecular organization of model membranes, several fluorescent probes, differing in their bilayer location and responsiveness to membrane perturbations, have been recruited as reporter molecules, viz. Prodan and DMC, residing at lipid–water interface, and pyrene and DPH, distributing in nonpolar core of a lipid bilayer (Fig. 1).

2. Materials and methods

2.1. Chemicals

Chicken egg white lysozyme and pyrene were purchased from Sigma (St. Louis, MO, USA).

1-Palmitoyl-2-oleoyl-*sn*-glycero-3-phosphocholine (PC), 1-palmitoyl-2-oleoyl-*sn*-glycero-3-phospho-*rac*-glycerol (PG) and cholesterol (Chol) were from Avanti Polar Lipids (Alabaster, AL). 4-Dimethylaminochalcone (DMC) was from Zonde (Latvia). Prodan (6-propionyl-2-dimethylaminonaphthalene) was from Invitrogen Molecular Probes (Eugene, OR, USA). 1,6-Diphenyl-1,3,5-hexatriene (DPH) was from EGA Chemie (Steinheim, Germany), and gel Toyopearl HW-60F was from Toyo Soda (Japan).

2.2. Preparation of lipid vesicles

Large unilamellar vesicles were prepared by extrusion from PC mixtures with PG (10 or 20 mol%) or Chol (30 mol%). A thin lipid film was first formed from the lipid mixtures in chloroform by removing the solvent under a stream of nitrogen. The dry lipid residues were subsequently hydrated with 5 mM sodium phosphate buffer, pH 7.4 at room temperature to yield lipid concentration of 1 mM. Thereafter, the sample was subjected to 15 passes through a 100 nm pore size polycarbonate filter (Millipore, Bedford, USA), yielding liposomes of desired composition. Hereafter, liposomes containing 10 and 20 mol% PG or 30 mol% Chol are referred to as PG_{10}, PG_{20} and $Chol_{30}$, respectively.

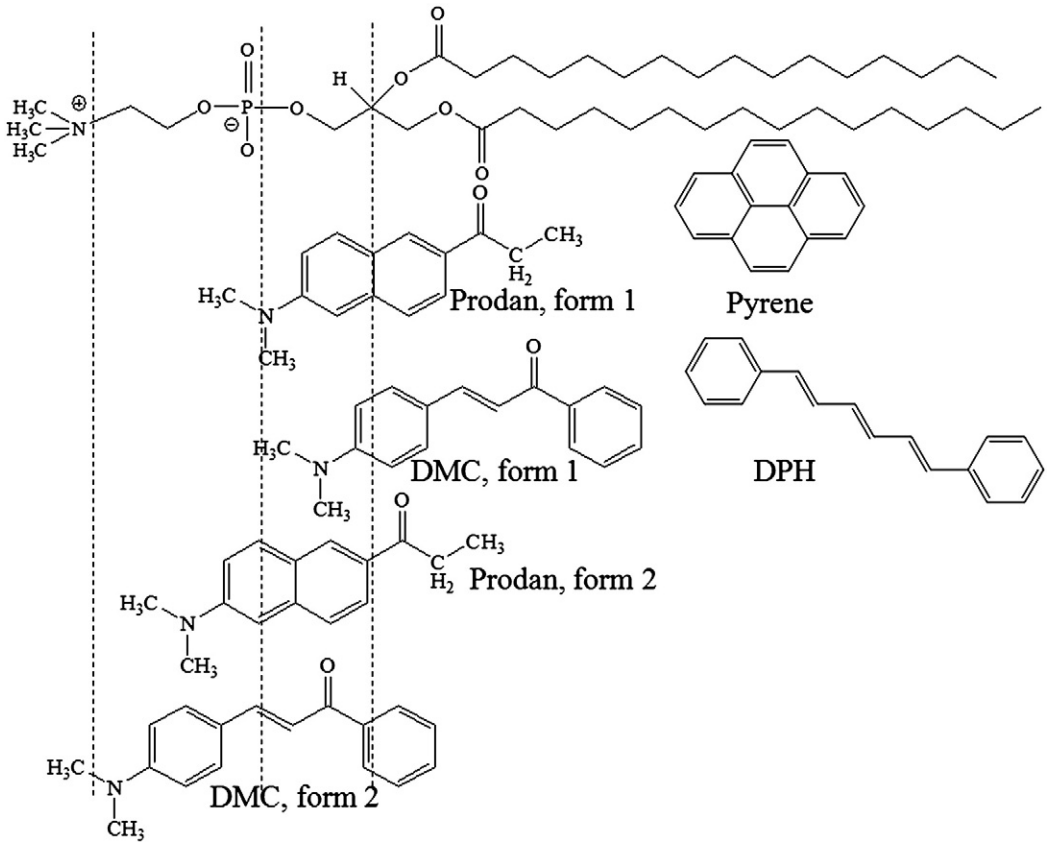

Fig. 1. Schematic representation of the location of Prodan, DMC, pyrene and DPH in a lipid bilayer.

2.3. Preparation of lysozyme aggregates

The reaction of lysozyme fibrillization was initiated using the approach developed by Holley and coworkers [26]. Protein solutions (3 mg/ml) were prepared by dissolving lysozyme in deionized water with subsequent slow addition of ethanol to a final concentration 80%. Next, the samples were subjected to constant agitation at ambient temperature. Protein fibrillization kinetics was measured by monitoring the changes in Thioflavin T fluorescence at 483 nm (Fig. 2).

For fluorescence measurements the aliquots of lysozyme solution (typically 20 μl) were withdrawn from agitated batch at the end of lag-phase (tenth day of the fibrillization reaction) and added to liposomes, preincubated with fluorescent probes. Analysis of aggregated protein samples used in fluorescence measurements by size-exclusion chromatography on a Toyopearl HW-60F column revealed the presence of lysozyme octamers, 20-mers and small fraction of dimers (Fig. 2, inset). In an analogous manner, we confirmed the monomeric nature of water-dissolved non-aggregated lysozyme (elution volume ~25.2 ml) used in comparative control experiments.

2.4. Fluorescence measurements

Steady-state fluorescence spectra were recorded with LS-55 spectrofluorometer equipped with a magnetically stirred, thermostated cuvette holder (Perkin-Elmer Ltd., Beaconsfield, UK). Fluorescence measurements were performed at 20 °C using 10 mm path-length quartz cuvettes. Emission spectra were recorded with excitation wavelengths of 340 nm (pyrene), 350 nm (Prodan) or 420 nm (DMC). Excitation and emission band passes were set at 10/10 nm (Prodan, DMC) and 5/2.5 nm (pyrene). The probe concentration was determined spectrophotometrically, using the extinction coefficients $\varepsilon_{337}=5.04\times10^4$ $M^{-1}cm^{-1}$ (pyrene), $\varepsilon_{360}=1.8\times10^4$ $M^{-1}cm^{-1}$ (Prodan), and $\varepsilon_{418}=3.5\times10^4$ $M^{-1}cm^{-1}$ (DMC).

To quantify Prodan partitioning into lipid phase fluorescence intensity increase ($\Delta I=I_L-I_W$) was represented as [27]:

$$\Delta I=\frac{K_pV_L(I_{max}-I_W)}{1+K_pV_L} \tag{1}$$

where I_L is the fluorescence intensity observed in the liposome suspension at a certain lipid concentration C_L, I_W is the probe fluorescence intensity in buffer, I_{max} is the limit fluorescence in the lipidic environment, K_p is the dye partition coefficient defined as:

$$K_p=\frac{N'_LV_W}{N'_WV_L} \tag{2}$$

here N'_L, N'_W are the moles of the dye in the lipid and aqueous phases, respectively; V_L , V_W are the volumes of these phases. The volume of lipid phase was calculated as:

$$V_L=N_AC_L\sum v_if_i \tag{3}$$

where C_L is the molar lipid concentration, f_i is mole fraction of the i-th bilayer constituent, v_i is its molecular volume taken as 1.58 nm^3 (PC, PG), and 0.74 nm^3 (Chol) [28]. For cholesterol-containing systems the condensing effect of this lipid was taken into account, so that the above v value was reduced by the factor 1.3 [10]. Under the employed experimental conditions (C_L< 1 mM) the V_L value is much less than total volume of the system ($V_t=1dm^3$), so that $V_W\approx V_t$.

Three-wavelength generalized polarization (3wGP) was determined as [29]:

$$3wGP=\frac{R_{12}-1}{R_{12}+1};\quad R_{12}=\frac{I_1k_{32}}{I_2k_{32}-I_3+I_1R_{31}};\quad k_{32}=I_{3W}/I_{2W};\quad R_{31}=I_{3M}/I_{1M} \tag{4}$$

where I_1, I_2, I_3 are Prodan fluorescence intensities at 420, 480 and 530 nm, respectively, subscripts W and M denote aqueous and membrane phases.

Deconvolution of fluorescence spectra of Prodan and DMC was performed with Origin 7.0 (OriginLab Corporation, Northampton, USA), with individual spectral components being approximated by a log-normal function.

The ratio of vibronic bands in pyrene fluorescence spectra ($R_{III}=I_I/I_{III}$) was calculated from the intensities at 372 nm (I_I) and 383 nm (I_{III}). The excimer-to-monomer fluorescence intensity ratio (E/M) was determined by measuring fluorescence intensity at monomer (392 nm) and excimer (468 nm) peaks.

Steady-state fluorescence anisotropy of DPH was measured using excitation and emission wavelengths of 350 and 450 nm, respectively, with excitation and emission band passes set at 10 nm. Stock solution of DPH was prepared in tetrahydrofurane. To incorporate the probe into lipid bilayers, liposomal suspensions were incubated with DPH for 30 min at 25 °C. Lipid concentration was 770 μM, and DPH concentration was 3.9 μM. Acyl chain order parameter was calculated from DPH anisotropy data acquired at protein concentration 3.1 μM.

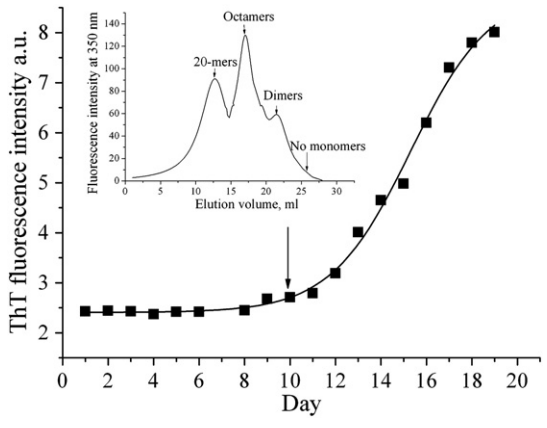

Fig. 2. Lysozyme fibrillazition kinetics monitored by measuring Thioflavin T fluorescence at 483 nm. Thioflavin T concentration was 10 μM. Shown in inset are the results of size-exclusion chromatography of the sample withdrawn at 10th day of lysozyme fibrillization.

3. Results

3.1. Bilayer modifications detected by Prodan

Fluorescent membrane probe Prodan is featured by high sensitivity to polarity and packing properties of lipid bilayer [30,31]. Numerous evidence indicates that Prodan emission spectra in model and natural membranes are composed of two bands corresponding to the probe molecules occupying different locations across a lipid bilayer [29,32]. Emission maxima of two spectral components (λ^1_{max},λ^2_{max}) were attributed to the probe molecules residing in i) low polar environment at the boundary between hydrophilic and hydrophobic bilayer regions, around glycerol backbone and initial acyl chain carbons (λ^1_{max} ~430–440 nm) and ii) high polar environment in the vicinity of phosphates (λ^2_{max} ~480–490 nm) or choline groups (λ^2_{max}~500–510 nm) [33]. Allowing for Prodan solubility in water our experimental strategy involved several consecutive steps: i) quantitative characterization of the probe partitioning between aqueous phase and liposomal membranes; ii) evaluation of the contribution of Prodan emission in buffer and reconstruction of the probe fluorescence spectra in a lipid

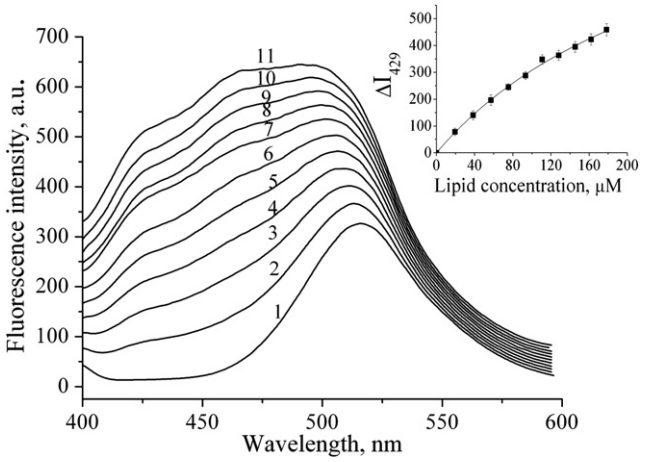

Fig. 3. Prodan fluorescence spectra in PC liposomes. Lipid concentration, μM: 1–0, 2–19, 3–38, 4–57, 5–75, 6–93, 7–111, 8–128, 9–145, 10–162, and 11–178. Prodan concentration was 0.09 μM. Shown in inset is the isotherm of Prodan binding to PC bilayer.

environment from its total emission; iii) deconvolution of fluorescence spectra of membrane-bound probe into components; iv) analysis of Prodan spectral data by three-wavelength generalized polarization method.

As demonstrated in Fig. 3, Prodan partitioning into lipid phase is accompanied by the increase of fluorescence intensity, short-wavelength shift of emission maximum and broadening of the emission spectra. The results of the probe fluorimetric titration with liposomes were quantitatively interpreted in terms of the aforementioned partition model. To derive the dye partition coefficients for different lipid systems the experimental dependencies $\Delta I(C_L)$ (Fig. 3, inset) were approximated by Eq. (3). The recovered K_P values (Table 1) suggest that Prodan affinity for liposomal membranes increases upon inclusion of PG or Chol into PC bilayer. The latter finding is in accord with the data of Bondar and Rowe, who showed that Prodan distribution into lipid phase significantly enhances in the presence of cholesterol [31]. Determination of partition coefficients (Table 1) allowed us to estimate the amount of the probe remaining in aqueous phase and to separate the contributions of membrane-bound and free species to the measured fluorescence spectra (Fig. 4, A). Next, as illustrated in Fig. 4, B and C, Prodan fluorescence spectra in a lipid environment were deconvoluted into two bands, whose emission maxima appeared to fall in the range 435–441 nm (λ^1_{max}) and 488–508 nm (λ^2_{max}). Relative integral intensity of the short-wavelength peak (R_1) rises in the presence of lysozyme oligomers, with the magnitude of this effect being most pronounced (R_1 increase by ~20%) for PG_{10} and PG_{20} liposomes (Table 2). On the contrary, monomeric lysozyme does not exert influence on this parameter, with the exception of R_1 increase by ~8% in PG_{20} liposomes. The above tendencies in R_1 behavior manifested themselves in the trends of three-wavelength generalized polarization (3*wGP*), another parameter derived here from the Prodan fluorescence spectra. This parameter has been introduced by Krasnowska et al. to allow for incomplete partitioning of Prodan into the lipid phase and eliminate the contribution of the probe free in buffer to the measured fluorescence signal [29]. Depending on the ratio of relative intensities of blue- and red-edge spectral components, 3*wGP* can be

Table 1
Partition coefficients for Prodan distribution between aqueous phase and liposomal membranes.

System	PC	PC/PG (9:1)	PC/PG (4:1)	PC/Chol (7:3)
Partition coefficient	$(1.9\pm0.2)\times10^3$	$(4.5\pm0.6)\times10^3$	$(5.3\pm0.8)\times10^3$	$(5.5\pm0.6)\times10^3$

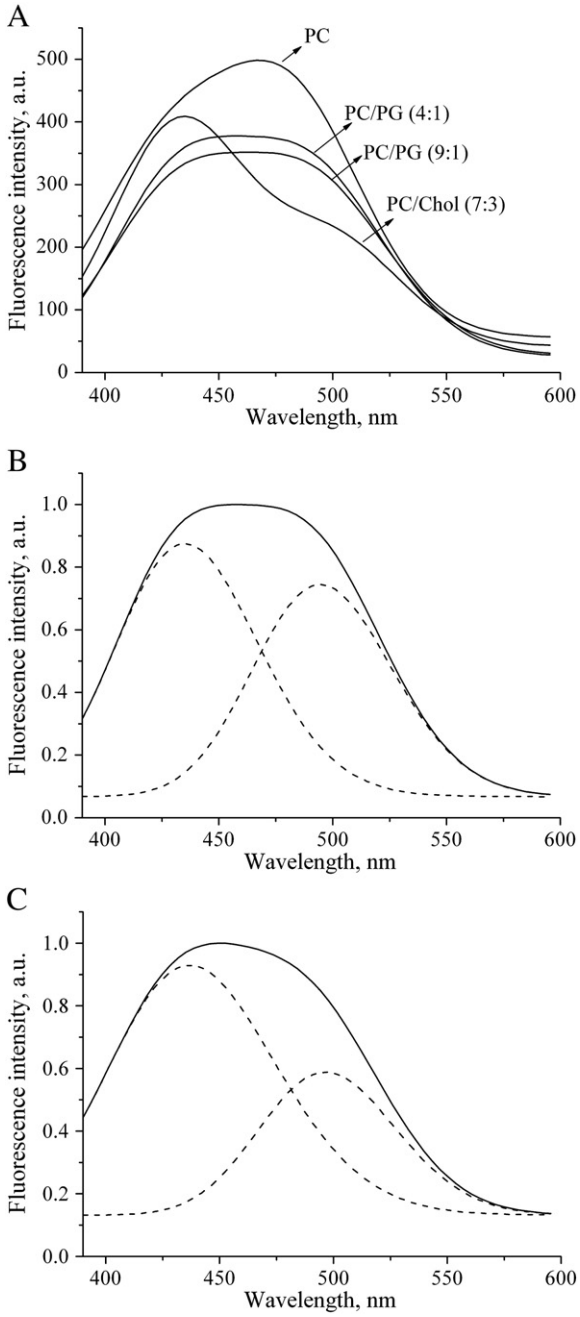

Fig. 4. Prodan emission spectra obtained after subtraction of the fluorescence signal from free probe for different types of liposomes (A). Deconvolution of Prodan fluorescence spectra in PC:PG (4:1) liposomes into two components in the absence (B) and presence (C) of lysozyme oligomers. Protein concentration was 3.1 μM, lipid concentration was 174 μM, and Prodan concentration was 0.17 μM.

Table 2
Effect of oligomeric lysozyme on spectral parameters of Prodan and DMC.

System	Prodan		DMC	
	R_1	3*wGP*	R_1	Integral intensity
PC	Increase (9%)	Increase (30%)	Increase (9%)	Increase (20%)
PC/PG (9:1)	Increase (20%)	Increase (34%)	Increase (11%)	Increase (21%)
PC/PG (4:1)	Increase (22%)	Increase (57%)	Increase (4%)	Increase (25%)
PC/Chol (7:3)	NC	NC	NC	NC

NC, no statistically significant change. Percentages are given for protein concentration 3.1 μM.

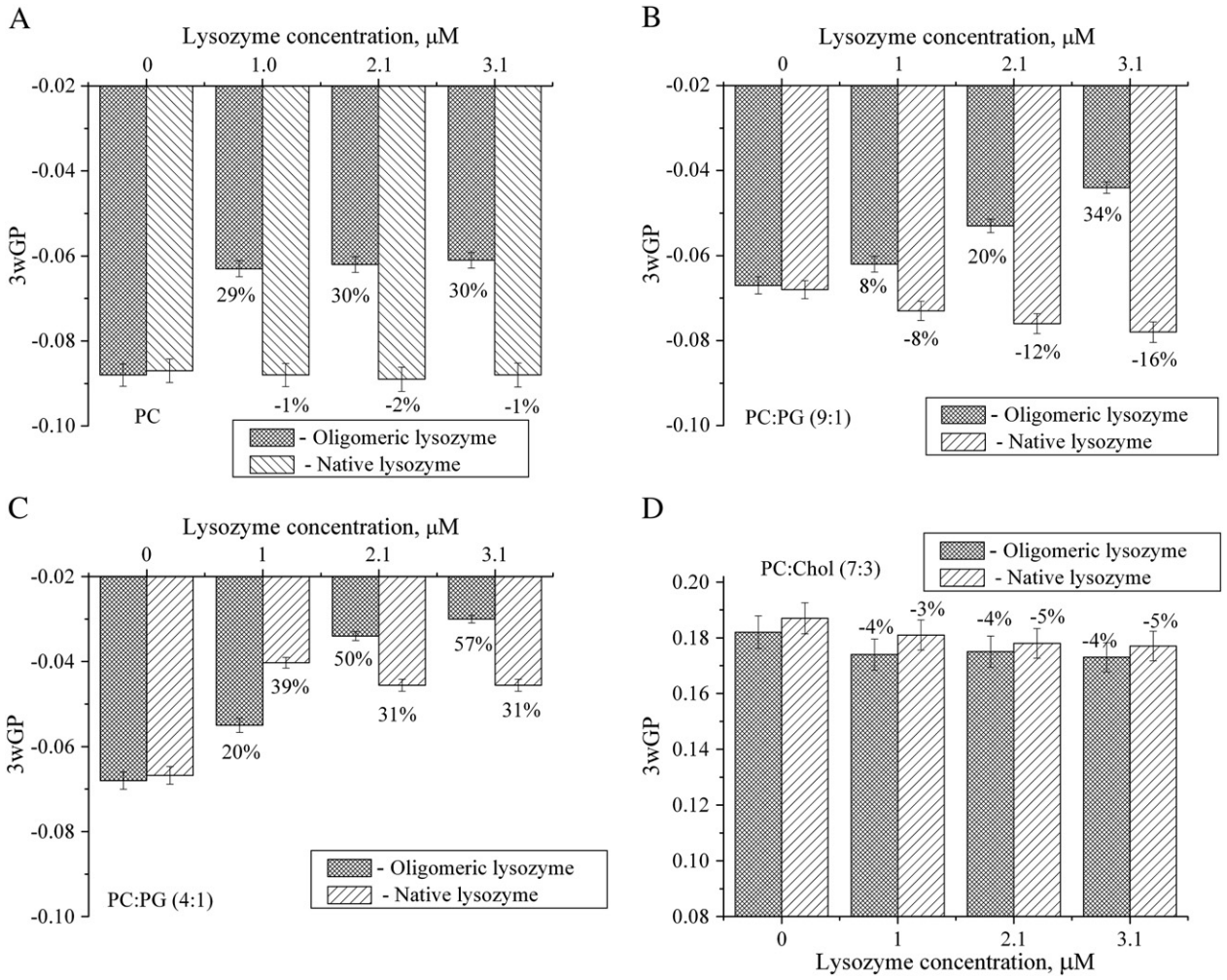

Fig. 5. Three-wavelength generalized polarization (3*wGP*) calculated from Prodan emission spectra in PC (A), PC:PG (9:1) (B), PC:PG (4:1) (C), and PC:Chol (7:3) (D). Figures indicate the percentage of 3*wGP* changes relative to protein-free control.

negative (red-edge component is prominent) or positive (blue-edge component is prominent).

As seen in Fig. 5, in PC, PG_{10} and PG_{20} liposomes 3*wGP* attain negative values reflecting the prevalence of probe species located in a more polar environment, while an opposite situation is observed for $Chol_{30}$ liposomes, in which the predominance of Prodan molecules occupying less polar membrane sites manifests itself in positive 3*wGP* value. Upon the addition of oligomeric lysozyme this parameter exhibited marked increase in PC, PG_{10} and PG_{20} liposomes and slight decrease in $Chol_{30}$ system. On the contrary, 3*wGP* changes brought about by monomeric lysozyme appear to lie beyond the experimental error only for PG_{10} (3*wGP* decrease) and PG_{20} (3*wGP* increase) liposomes.

3.2. Membrane effects probed by DMC

Shown in Fig. 6, A are typical fluorescence spectra of DMC observed in lipid and lysozyme–lipid systems. Similar to Prodan, deconvolution of DMC spectra revealed two populations of membrane-bound probe occupying less polar (λ^1_{max} ~496–509 nm) and more polar (λ^2_{max} ~531–563 nm) locations across lipid bilayer (Fig. 6, B and C). As shown in Table 2, oligomeric lysozyme brought about the rise in overall fluorescence intensity (~20%) in PC, PG_{10} and PG_{20} systems accompanied by the increase of relative integral intensity (~10%) of less polar spectral component (R_1) in PC and PG_{10} liposomes. In contrast, no changes in λ^1_{max}, λ^2_{max} and R_1 were detected in the presence of monomeric protein, while fluorescence intensity exhibited increase (~12%) in PG_{20} liposomes and decrease (~8%) in $Chol_{30}$ liposomes.

3.3. Bilayer modifications elicited by pyrene and DPH

Along with Prodan and DMC, capable of sensing perturbations in polar membrane region, in the present study we employed pyrene and DPH, classical fluorescent probes commonly used to follow the changes in nonpolar membrane core. Fig. 7 shows typical fluorescence spectra of pyrene in the investigated systems. These spectra exhibit a well-defined vibronic structure attributed to the probe monomer emission (vibronic bands numbered I–V from the lowest wavelength). Relative intensities of vibronic transitions are featured by distinct dependence on solvent polarity ("Ham effect") [34]. For instance, intensity ratio $R_{III} = I_I/I_{III}$ is reported to be 1.96 in water, while in the solvents of lower polarity this ratio tends to decrease, reaching the value 0.6 in n-hexane [35].

Both monomeric and oligomeric lysozyme exerted no influence on R_{III} value, suggesting that the degree of hydration in acyl group region remained virtually unchanged. On the contrary, another parameter recovered here from pyrene spectra, excimer-to-monomer fluorescence intensity ratio (E/M), showed a clear decrease upon protein addition to all types of liposomes, with the magnitude of this effect being markedly more pronounced for lysozyme oligomers

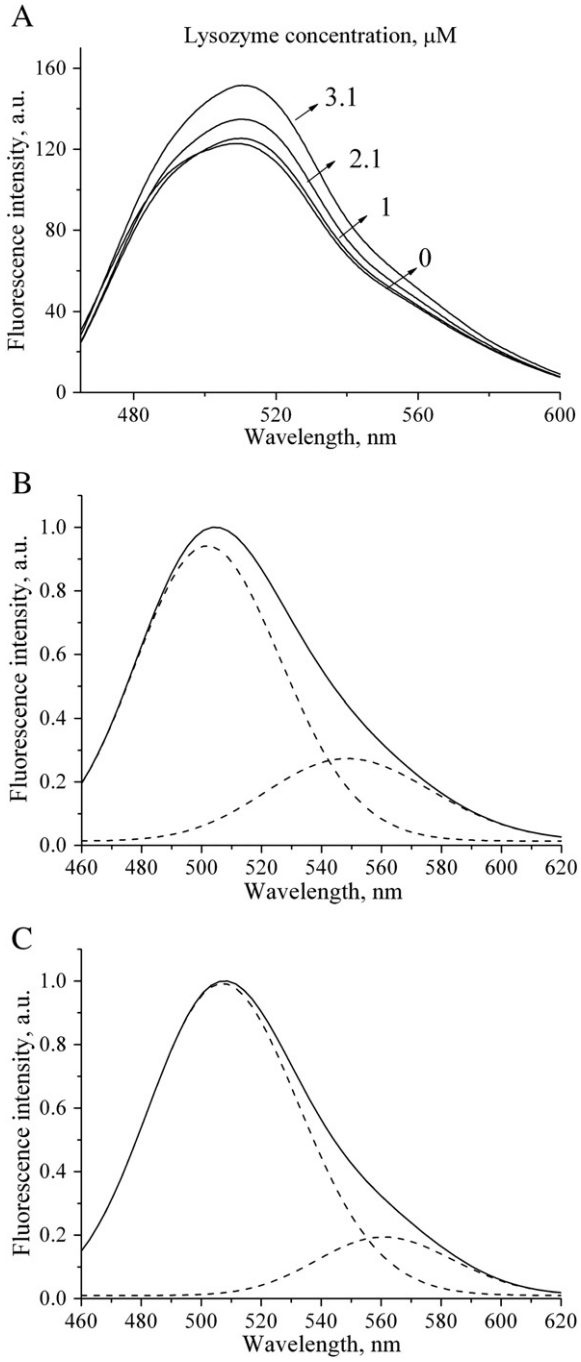

Fig. 6. Effect of oligomeric lysozyme on DMC fluorescence spectra in PC liposomes (A). Deconvolution of DMC fluorescence spectra in PC:PG (4:1) liposomes into two components in the absence (B) and presence (C) of lysozyme oligomers. Protein concentration was 3.1 μM, lipid concentration was 69 μM, and DMC concentration was 0.17 μM.

(Fig. 8). The amount of excimers is determined by the rate of the probe lateral diffusion, which, in turn, is a function of membrane fluidity, or, more strictly speaking, free volume of a lipid bilayer [25]. The observed lowering of pyrene excimerization led us to assume that bilayer free volume tends to decrease in the presence of lysozyme. To check the validity of this assumption, we conducted a series of experiments with DPH, another probe located in hydrophobic membrane core, whose anisotropy depends on ordering of acyl chains. It has been demonstrated that enhanced ordering of acyl chains is correlated with decrease in free volume of lipid bilayer [36]. According to Pottel et al. acyl chain order parameter (S) and

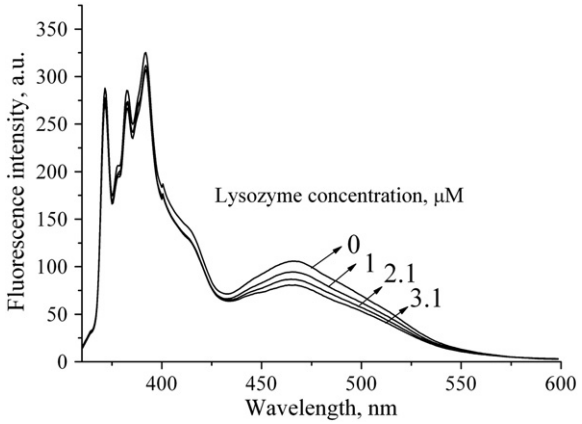

Fig. 7. Effect of oligomeric lysozyme on the pyrene fluorescence spectra in PC liposomes. Lipid concentration was 24 μM, and probe concentration was 0.6 μM.

steady-state fluorescence anisotropy of DPH (r_s) are related by the following analytical expression [37]:

$$S = \frac{\left[1-2(r_s/r_o) + 5(r_s/r_o)^2\right]^{1/2} - 1 + r_s/r_o}{2(r_s/r_o)} \quad (5)$$

here r_o is fundamental anisotropy of DPH (0.362). Using Eq. (5), we calculated acyl chain order parameter for lysozyme–lipid systems under study (Table 3). The increase of this parameter revealed for PG_{10} and PG_{20} liposomes, which can be regarded as an additional argument in favor of the above hypothesis about lysozyme ability to reduce free volume of lipid bilayer. In contrast to E/M, lysozyme exerted no influence on S value in PC and $Chol_{30}$ liposomes. This may result from the difference in lipid-to-protein molar ratio (L/P) employed in pyrene excimerization (L/P~8) and DPH anisotropy measurements (L/P~250).

4. Discussion

The present study revealed that bilayer composition plays a significant role in determining the nature of membrane perturbations caused by pre-fibrillar aggregates of lysozyme. Under the employed lipid-to-protein molar ratios, oligomeric lysozyme turned out to display much more membranotropic activity than its monomeric counterpart. The observed changes in the Prodan fluorescence spectra (Table 2) can be interpreted in terms of environmental polarity, lipid molecular packing and probe redistribution between membrane sites differing in chemical nature of phospholipid groups, extent of hydration and solvent dynamics in fluorophore's surrounding. The integral fluorescence intensity ($I \sim C_1Q_1 + C_2Q_2$) is proportional to the concentrations (C_1,C_2) and quantum yields (Q_1,Q_2) of two probe species located presumably at the level of phosphate groups (λ^2_{max} ~489–508 nm) and glycerol backbone (λ^1_{max} ~435–441 nm). The enhancement of the first spectral component (R_1 increase) recovered for PC, PG_{10} and PG_{20} systems may come from the increase of Q_1 and/or C_1. The rise in Q_1 can be explained by the decreased concentration of water molecules in the vicinity of the glycerol backbone, while the increase in C_1 implies that incorporation of the aggregated protein species into the membrane interior promotes squeezing of a part of fluorophores out of the phosphate group region and accommodation of the displaced Prodan molecules in less polar sites embracing glycerol backbone and initial acyl chain carbons. The latter possibility stems from the reported correlation between bilayer location of this probe and molecular packing of lipids. Specifically, it has been demonstrated that Prodan molecules tend to occupy more polar membrane sites as the cross-sectional area of lipid head groups becomes larger [33]. In view of this finding, the most pronounced increase of R_1

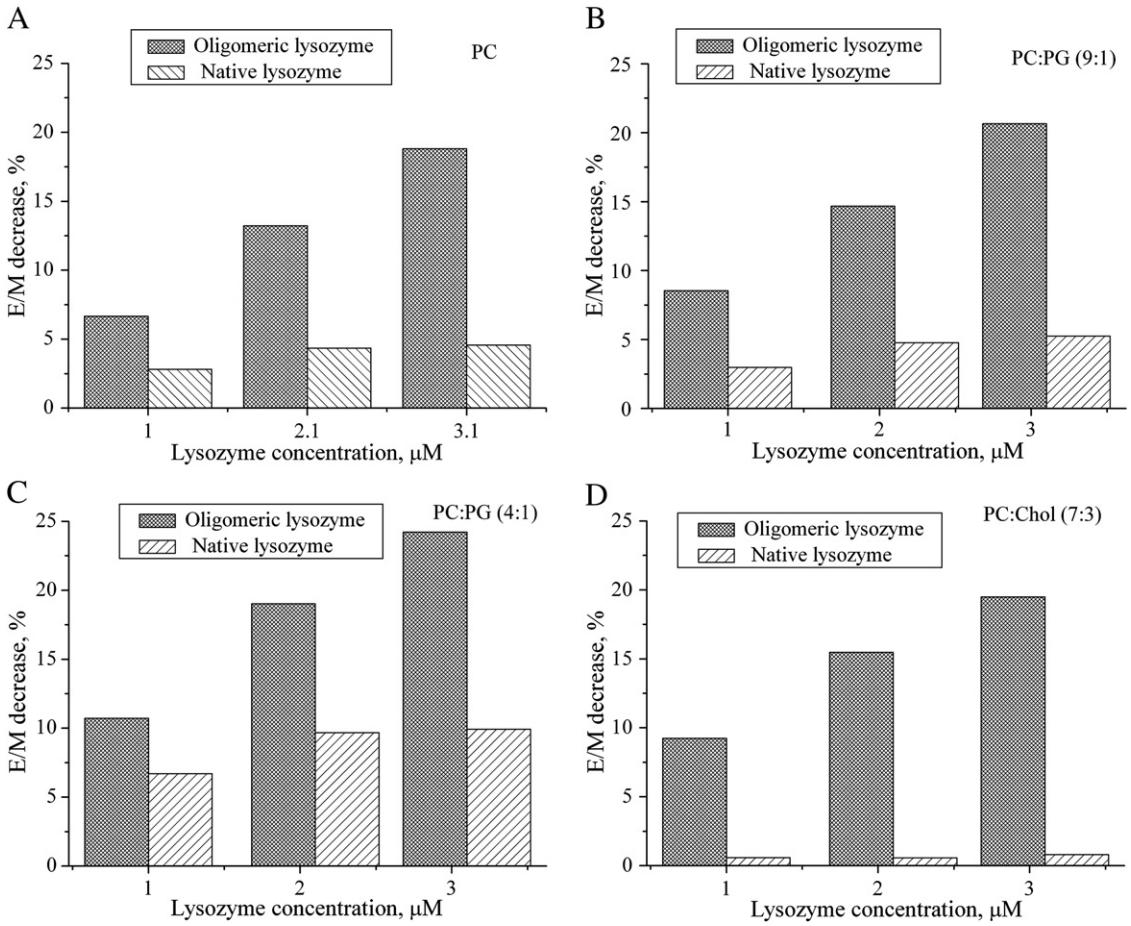

Fig. 8. The changes in pyrene excimer-to-monomer fluorescence intensity ratio produced by oligomeric and native lysozyme in PC (A), PC:PG (9:1) (B), PC:PG (4:1) (C), and PC:Chol (7:3) (D) liposomes.

found in the PG_{10} and PG_{20} systems could hardly be attributed to the relocation of the probe molecules from phosphate groups to the glycerol backbone region (C_1 increase), because the average headgroup spacing seems to be higher in PG-containing liposomes due to enhanced charge–charge repulsion.

Analogous rationales seem to be applicable while interpreting spectral effects observed with DMC, another polarity-sensitive probe, containing alkylamino and carbonyl groups (Fig. 1). Similar to Prodan, DMC tends to distribute between two membrane sites located presumably at the level of phosphate groups and glycerol backbone, as schematically depicted in Fig. 1. Since DMC fluorescence is strongly quenched by water molecules, it displays high sensitivity to the degree of membrane hydration [38]. In view of this, the observed increase of relative contribution of less polar DMC form to overall spectrum, together with the rise in integral fluorescence intensity (Table 2) corroborate the above idea about bilayer dehydration under the influence of oligomeric lysozyme. In this context it is noteworthy that our data is not in conflict with the reported ability of Aβ oligomers to affect the membrane dielectric properties by inducing lateral heterogeneity in the bilayers, but not by the increasing the degree of membrane hydration [17].

Table 3
Effect of lysozyme on acyl chain order parameter.

System	PC	PC/PG (9:1)	PC/PG (4:1)	PC/Chol (7:3)
Without protein	0.51	0.50	0.39	0.50
+ Protofibrillar lysozyme	0.50	0.65	0.62	0.49
+ Monomeric lysozyme	0.50	0.57	0.48	0.50

Remarkably, neither Prodan nor DMC reported any changes in polar region of $Chol_{30}$ liposomes in the presence of oligomeric lysozyme (Table 2). It is well known that cholesterol per se can profoundly modify the lipid bilayer properties. In the liquid-crystalline lipid phase cholesterol can give rise to i) an increase of headgroup separation [39]; ii) increased freedom of motion of phosphorylcholine moiety [39]; iii) enhanced headgroup hydration [40]; iv) reduced content of the acyl chain *gauche* conformations [41]; v) tighter lateral packing of hydrocarbon chains (condensing effect) [42]. Cholesterol hydrophobic moiety is buried into the nonpolar membrane core, while its OH-group sticks out into the polar region, forming a hydrogen bond with carbonyl group of the glycerol backbone [43]. Due to the presence of the carbonyl group in the structure of both Prodan and DMC, these probes are capable of hydrogen bonding to cholesterol hydroxyl group. This kind of specific interactions may render Prodan and DMC insensitive to membrane modifications. However, while recruiting another probe located at the hydrophilic/hydrophobic boundary, DSP-12, which is devoid of H-bonding capability, we failed to detect any lysozyme-induced changes in PC/Chol bilayers. This allowed us to conclude that perturbing effect of oligomeric protein on the polar membrane region is prevented by cholesterol inclusion. Our results are in harmony with the findings reported elsewhere. Particularly, cholesterol was demonstrated to protect primary cortical neurons from neurotoxicity of soluble oligomeric Aβ, by modulating the physical properties of lipid bilayer. Model membrane studies showed that increase of cholesterol content inhibited aggregation and fusion of liposomes induced by Aβ(1–40) peptide [44].

To obtain more comprehensive information on the mechanisms of membrane modification produced by oligomeric lysozyme, polar

fluorescent probes Prodan and DMC were complemented by non-polar probes pyrene and DPH. Pyrene is a polycyclic aromatic compound which is primarily distributed in the region of 4–13 carbons, with its principal long axis being aligned along bilayer normal [45]. Pyrene excimerization occurring in a lipid bilayer is commonly regarded as a diffusion-controlled process which can be analyzed in terms of the free volume model [46]. This model describes diffusion of membrane constituents or guest molecules as a three-step process: i) formation of dynamic defects (kinks) in the acyl chains followed by opening of the cavities in a lipid monolayer; ii) jump of diffusing molecules into the cavities coupled with the void generation; iii) sealing the voids by movement of defects along the adjacent hydrocarbon chains. The appearance of dynamic defects in a membrane interior is associated with *trans-gauche* isomerization of acyl chains initiated by thermal motion and packing constraints. Membrane free volume, produced by lateral displacements of hydrocarbon chains after kink formation, is defined by the difference between effective and van der Waals volumes of lipid molecules. Lysozyme-induced reduction in bilayer free volume inferred from the observed decrease of E/M ratio may be rationalized on a basis of the lowered rate of *trans-gauche* isomerization of hydrocarbon chains. Likewise, bilayer condensation may result from the membrane dehydration in the acyl group region. However, the latter possibility contradicts the absence of any changes in polarity-sensitive paramer R_{III} upon lysozyme-membrane interaction.

Comparison of the data presented in Fig. 8, indicates that the magnitude of bilayer perturbations introduced by oligomeric lysozyme in non-polar membrane region is slightly dependent on membrane composition. For instance, at maximum lysozyme concentration (3.1 μM) the decrease of excimerization extent was ca. 20% in PC, PG_{10} and $Chol_{30}$ liposomes and only slightly greater (ca. 25%) in PG_{20} liposomes. Lysozyme in its monomeric form bears a net positive charge over a broad pH range (p*I* ca. 11.0). Evidently, some part of the charged groups would be exposed to solvent in the aggregated protein, enhancing oligomer affinity for negatively charged lipid bilayers. However, as judged from the data presented here, electrostatic interactions do not play a determining role in the bilayer-modifying propensity of oligomeric lysozyme. Otherwise, hydrophobic interactions seem to be essential for reorganization of membrane architecture in response to the binding of protein pre-fibrillar aggregates. In keeping with this observation are the results reported elsewhere. More specifically, analysis of the fluorescence responses of bis-ANS and DPH indicated that aggregated Aβ amyloid peptide decreases fluidity of the model membranes in a manner, correlating with surface hydrophobicity of the aggregates [47]. Moreover, Aβ aggregates were found to increase the ordering of acyl chains in the bilayers from anionic, cationic or zwitterionic phospholipids, with little or no alterations in the headgroup region, pointing out that electrostatic interactions are not critical for the perturbation of membrane structure [15]. As evidenced by the dye release assay study into the membrane effects of sinuclein oligomers, bilayer composition changes resulting in an increased lipid headgroup spacing render the lipid vesicles more vulnerable to disruption suggesting that oligomer–membrane interactions are modulated by the accessibility of the bilayer hydrocarbon core [18].

Numerous studies offer insights into membrane-modifying effects of amyloid intermediates. Clearly, the processes initiated by amyloid intermediates in natural membranes are much more complex than those in model membranes. In natural membranes aggregated species are most likely to act via diverse sites and perturbations of lipid bilayer represent only one of the multiple operative mechanisms. For instance, lysozyme protofibrils and mature fibrils were found to exert disruptive effect on erythrocyte membranes involving aggregation of membrane proteins through intermolecular disulfide cross-linking [48]. Lysozyme oligomers induced apoptosis-like death of neurons, fibroblasts and neuroblastoma cells [49,50]. Amyloid Aβ peptide was shown to trigger erythrocyte death followed by scrambling of the cell membrane [51] and exhibited ability to reduce fluidity of hippocampal membranes in hydrophobic region [52], the effect being similar to that observed in model membranes [15]. The extent to which proteins or other membrane constituents determine the toxic effects of pre-fibrillar aggregates and modulate their bilayer-modifying propensity remains to be elucidated in future investigations both with model and natural membranes.

In summary, principal findings of the present study can be outlined as follows.

(1) Fluorescence responses of polarity-sensitive probes Prodan and DMC located at the lipid–water interface provides evidence of a decrease of glycerol backbone hydration in neutral (PC) and negatively charged (PC/PG) lipid bilayers under the influence of oligomeric lysozyme.
(2) The ability of lysozyme oligomers to modify interfacial membrane region is hampered by cholesterol.
(3) As judged from pyrene excimerization and DPH anisotropy measurements, aggregated protein gives rise to the tighter packing of lipid acyl chains, with the magnitude of this effect being insignificantly dependent on the presence of anionic phospholipid (PG) or cholesterol.
(4) Membrane-modifying propensity of aggregated lysozyme is much higher than that of its monomeric counterpart.

Although translation of the above findings into the membrane effects of lysozyme oligomers in vivo is not immediate, they may prove of significance in creating a solid background for understanding membrane-related mechanisms accounting for cytotoxicity of pre-fibrillar protein assemblies.

Acknowledgements

This work was supported by the grants from European Social Fund (project number 2009/0205/1DP/1.1.1.2.0/09/APIA/VIAA/152), the Science and Technology Center in Ukraine (project number 4534) and Fundamental Research State Fund (project number F.28.4/007). V. T. gratefully acknowledges an award by Human Frontier Science Program. The authors are indebted to referees for valuable remarks.

References

[1] M. Stefani, Protein folding and misfolding on surfaces, Int. J. Mol. Sci. 9 (2008) 2515–2542.
[2] M. Stefani, Protein misfolding and aggregation: new examples in medicine and biology of the dark side of the protein world, Biochim. Biophys. Acta 1739 (2004) 5–25.
[3] B. Caughey, P.T. Lansbury, Protofibrils, pores, fibrils, and neurodegeneration: separating the responsible protein aggregates from the innocent bystanders, Annu. Rev. Neurosci. 26 (2003) 267–298.
[4] N. Arispe, E. Rojas, H. Pollard, Alzheimer's disease amyloid beta protein forms calcium channels in bilayer membranes: blockade by tromethamine and aluminium, Proc. Natl. Acad. Sci. U.S.A. 89 (2003) 10940–10944.
[5] T. Squier, Oxidative stress and protein aggregation during biological aging, Exp. Gerontol. 36 (2001) 1539–1550.
[6] B. Tabner, S. Turnbull, O. El-Agnaf, D. Allsop, Formation of hydrogen peroxide and hydroxyl radicals from Aβ and α-synuclein as a possible mechanism of cell death in Alzheimer's disease and Parkinson's disease, Free Radic. Biol. Med. 32 (2002) 1076–1083.
[7] E. Sparr, M.F.M. Engel, D.V. Sakharov, M. Sprong, J. Jacobs, B. de Kruijf, J.W.M. Hoppener, J.A. Killian, Islet amyloid polypeptide-induced membrane leakage involves uptake of lipids by forming amyloid fibers, FEBS Lett. 577 (2004) 117–120.
[8] J.D. Knight Test, A.D. Miranker, Phospholipid catalysis of diabetic amyloid assembly, J. Mol. Biol. 341 (2004) 1175–1187.
[9] R. Byström, C. Aisenbrey, T. Borowik, M. Bokvist, F. Lindström, M. Sani, A. Olofsson, G. Gröbner, Disordered proteins: biological membranes as two-dimensional aggregation matrices, Cell Biochem. Biophys. 52 (2008) 175–189.
[10] E. Giannakis, J. Pacifico, D.P. Smith, L.W. Hung, C.L. Masters, R. Cappai, J.D. Wade, K.J. Barnham, Dimeric structures of α-synuclein bind preferentially to lipid membranes, Biochim. Biophys. Acta 1778 (2008) 1112–1119.
[11] D.H.J. Lopes, A. Meister, A. Gohlke, A. Hauser, A. Blume, R. Winter, Mechanism of IAPP fibrillation at lipid interfaces studied by infrared reflection absorption spectroscopy (IRRAS), Biophys. J. 93 (2007) 3132–3141.

[12] D.P. Smith, D.J. Tew, A.F. Hill, S.P. Bottomley, C.L. Masters, K.J. Barnham, R. Cappai, Formation of a high affinity lipid-binding intermediate during the early aggregation phase of α-synuclein, Biochemistry 47 (2008) 1425–1434.
[13] S. Dante, T. Haus, A. Brandt, N.A. Dencher, Membrane fusogenic activity of the Alzheimer's peptide Abeta(1–42) demonstrated by small-angle neutron scattering, J. Mol. Biol. 376 (2008) 393–404.
[14] A. Quist, I. Doudewski, H. Lin, R. Azimova, D. Ng, B. Frangine, B. Kagan, J. Ghiso, R. Lal, Amyloid ion channels: a common structural link for protein-misfolding disease, Proc. Natl. Acad. Sci. U.S.A. 102 (2005) 10427–10432.
[15] J.J. Kremer, D.J. Sklansky, R.M. Murphy, Profile of changes in lipid bilayer structure caused by β-amyloid peptide, Biochemistry 40 (2001) 8563–8571.
[16] D.H. Kim, J.A. Frangos, Effects of amyloid β-peptides on the lysis tension of lipid bilayer vesicles containing oxysterols, Biophys. J. 95 (2008) 620–628.
[17] G. Valincius, F. Heinrich, R. Budvytyte, D.J. Vanderah, D.J. McGillivray, Yu. Sokolov, J.E. Hall, M. Losche, Soluble amyloid β-oligomers affect dielectric membrane properties by bilayer insertion and domain formation: implications for cell toxicity, Biophys. J. 95 (2008) 4845–4861.
[18] B.D. van Rooijen, M.M.A.E. Claessens, V. Subramaniam, Lipid bilayer disruption by oligomeric α-synuclein depends on bilayer charge and accessibility of the hydrophobic core, Biochim. Biophys. Acta 1788 (2009) 1271–1278.
[19] A. Relini, S. Torrassa, R. Rolandi, A. Gliozzi, C. Rosano, C. Canale, M. Bolognesi, G. Plakoutsi, M. Bucciantini, F. Chiti, M. Stefani, Monitoring the process of HypF fibrillization and liposome permeabilization by protofibrils, J. Mol. Biol. 338 (2004) 943–957.
[20] C. Canale, S. Torrassa, P. Rispoli, A. Relini, R. Rolandi, A. Bucciantini, M. Stefani, A. Gliozzi, Natively folded Hypf-N and its early amyloid aggregates interact with phospholipid monolayers and destabilize supported lipid bilayers, Biophys. J. 91 (2006) 1–14.
[21] G. Anderluh, I. Gutierrez-Aguirre, S. Rabzelj, S. Ceru, N. Kopitar-Jerala, P. Macek, V. Turk, E. Zerovnik, Interaction of human stefin B in the prefibrillar oligomeric form with membranes. Correlation with cellular toxicity, FEBS J. 272 (2005) 3042–3051.
[22] M.B. Pepys, P.N. Hawkins, D.R. Booth, D.M. Vigushin, G.A. Tennent, A.K. Souter, N. Totty, O. Nguyen, C.C.F. Blake, C.J. Terry, T.G. Feest, A.M. Zalin, J.J. Hsuan, Human lysozyme gene mutations cause hereditary systemic amyloidosis, Nature 362 (1993) 553–557.
[23] J.J. Bergers, M.H. Vingerhoeds, L. van Bloois, J.N. Herron, L.H. Jassen, M.J. Fisher, D. Crommelin, The role of protein charge in protein–lipid interactions. pH-dependent changes of the electrophoretic mobility of liposomes through adsorption of water-soluble, globular proteins, Biochemistry 32 (1993) 4641–4649.
[24] O. Zschornig, G. Paasche, C. Thieme, N. Korb, A. Fahrwald, K. Arnold, Association of lysozyme with phospholipid vesicles is accompanied by membrane surface dehydration, Gen. Physiol. Biophys. 19 (2000) 85–101.
[25] V.M. Ioffe, G.P. Gorbenko, Lysozyme effect on structural state of model membranes as revealed by pyrene excimerization studies, Biophys. Chem. 114 (2005) 199–204.
[26] M. Holley, C. Eginton, D. Schaefer, L.R. Brown, Characterization of amyloidogenesis of hen lysozyme in concentrated ethanol solution, Biochem. Biophys. Res. Commun. 373 (2008) 164–168.
[27] N.C. Santos, M. Prieto, M.A.R.B. Castanho, Quantifying molecular partition into model systems of biomembranes: an emphasis on optical spectroscopic methods, Biochim. Biophys. Acta 1612 (2003) 123–135.
[28] V.G. Ivkov, G.N. Berestovsky, Dynamic structure of lipid bilayer, Nauka, Moscow, 1981.
[29] E.K. Krasnowska, E. Gratton, T. Parasassi, Prodan as a membrane surface fluorescence probe: partitioning between water and phospholipid phases, Biophys. J. 74 (1998) 1984–1993.
[30] J. Zeng, P.L.-G. Chong, Effect of ethanol-induced lipid interdigitation on the membrane solubility of Prodan, Acdan, and Laurdan, Biophys. J. 68 (1995) 567–573.
[31] O.P. Bondar, E.S. Rowe, Preferential interactions of fluorescent probe Prodan with cholesterol, Biophys. J. 76 (1999) 956–962.
[32] R. Hutterer, F.W. Schneider, H. Sprinz, M. Hof, Binding and relaxation behaviour of prodan and patman in phospholipid vesicles: a fluorescence and ^{1}H-NMR study, Biophys. Chem. 61 (1996) 151–160.
[33] M. Kusube, H. Matsuki, S. Kaneshina, Effect of pressure on the Prodan fluorescence in bilayer membranes of phospholipids with varying acyl chain lengths, Coll. Surf. B 42 (2005) 79–88.
[34] A. Nakajima, Solvent effect on the vibrational structure of the fluorescence and absorption spectra of pyrene, Bull. Chem. Soc. Jpn. 44 (1971) 3272–3277.
[35] D.S. Karpovich, G.J. Blanchard, Relating the polarity-dependent fluorescence response to vibronic coupling. Achieving a fundamental understanding of the *py* polarity scale, J. Phys. Chem. 99 (1995) 3951–3958.
[36] M. Kupiainen, E. Falck, S. Ollila, P. Niemelä, A.A. Gurtovenko, M.T. Hyvönen, M. Patra, M. Karttunen, I. Vattulainen, Free volume properties of sphingomyelin, DMPC, DPPC, and PLPC bilayers, J. Comput. Theor. Nanosci. 2 (2005) 401–413.
[37] H. Pottel, B.W. van der Meer, W. Herreman, Correlation between the order parameter and the steady-state fluorescence anisotropy of 1, 6-diphenyl-1, 3, 5-hexatriene and an evaluation of membrane fluidity, Biochim. Biophys. Acta 730 (1983) 181–186.
[38] G.E. Dobretsov, V.A. Petrov, Yu.A. Vladimirov, 4-dimethylaminochalcone and 3-methoxybenzanthrone as fluorescent probes to study biomembranes. II. Sensitivity of 4-dimethylaminochalcone to water molecules in the surface layer of a membrane, Stud. Biophys. 65 (1977) 181–187.
[39] M. Pasenkiewicz-Gierula, T. Rog, K. Kitamura, A. Kusumi, Cholesterol effects on the phosphatidylcholine bilayer polar region: a molecular simulation study, Biophys. J. 78 (2000) 1376–1389.
[40] D. Bach, I.R. Miller, Hydration of phospholipid bilayers in the presence and absence of cholesterol, Biochim. Biophys. Acta 1368 (1998) 216–224.
[41] T. Rog, M. Pasenkiewicz-Gierula, Cholesterol effects on the phosphatidylcholine bilayer nonpolar region: a molecular simulation study, Biophys. J. 81 (2001) 2190–2202.
[42] R.A. Demel, B. de Kruijff, The function of sterols in membranes, Biochim. Biophys. Acta 457 (1976) 109–132.
[43] C. Ho, S. Slater, C. Stubbs, Hydration and order in lipid bilayers, Biochemistry 34 (1995) 6188–6195.
[44] I. Sponne, A. Fifre, V. Koziel, T. Oster, J.L. Olivier, T. Pillot, Membrane cholesterol interferes with neuronal apoptosis induced by soluble oligomers but not fibrils of amyloid- β peptide, FASEB J. 838 (2004) 836–838.
[45] T.X. Xiang, B.D. Anderson, Influence of chain ordering on the selectivity of dipalmitoylphosphatidylcholine bilayer membranes for permeant size and shape, Biophys. J. 75 (1998) 2658–2671.
[46] E.W. Montroll, Random walks on lattices, J. Math. Phys. 10 (1969) 753–765.
[47] J.J. Kremer, M.M. Pallitto, D.J. Sklansky, R.M. Murphy, Correlation of beta-amyloid aggregate size and hydrophobicity with decreased bilayer fluidity of model membranes, Biochemistry 39 (2000) 10309–10318.
[48] B. Huang, J. He, J. Ren, X.Y. Yan, C.M. Zeng, Cellular membrane disruption by amyloid fibrils involved intermolecular disulfide cross-linking, Biochemistry 48 (2009) 5794–5800.
[49] M. Malisauskas, J. Ostman, A. Darinskas, V. Zamotin, E. Liutkevicius, E. Lundgren, L.A. Morozova-Roche, Does the cytotoxic effect of transient amyloid oligomers from common equine lysozyme in vitro imply innate amyloid toxicity? J. Biol. Chem. 280 (2005) 6269–6275.
[50] A.L. Gharibyan, V. Zamotin, K. Yanamandra, O.S. Moskaleva, B.A. Margulis, I.A. Kostanyan, L.A. Morozova-Roche, Lysozyme amyloid oligomers and fibrils induce cellular death via different apoptotic/necrotic pathways, J. Mol. Biol. 365 (2007) 1337–1349.
[51] J. Nicolay, S. Gatz, G. Liebig, E. Gulbins, F. Lang, Amyloid induced suicidal erythrocyte death, Cell. Physiol. Biochem. 19 (2007) 175–184.
[52] G.P. Eckert, N.J. Cairns, A. Maras, W.F. Gattaz, W.E. Müllera, Cholesterol modulates the membrane- disordering effects of beta-amyloid peptides in the Hippocampus: specific changes in Alzheimer's disease, Dement. Geriatr. Cogn. Disord. 11 (2000) 181–186.